Article

Laboratory Salinization of Brazilian Alluvial Soils and the Spectral Effects of Gypsum

Luis Clenio J. Moreira [1], Adunias dos Santos Teixeira [1] and Lênio Soares Galvão [2,*]

[1] Departamento de Engenharia Agrícola, Universidade Federal do Ceará (UFC), Caixa Postal 12.168, Fortaleza, CE 60450-760, Brazil; E-Mails: cleniojario@gmail.com (L.C.J.M.); adunias@ufc.br (A.S.T.)

[2] Instituto Nacional de Pesquisas Espaciais (INPE), Divisão de Sensoriamento Remoto, Caixa Postal 515, São José dos Campos, SP 12245-970, Brazil

* Author to whom correspondence should be addressed; E-Mail: lenio@dsr.inpe.br; Tel.: +55-12-3208-6443; Fax: +55-12-3208-6460.

Abstract: Irrigation-induced salinization is an important land degradation process that affects crop yield in the Brazilian semi-arid region, and gypsum has been used as a corrective measure for saline soils. Fluvent soil samples (180) were treated with increasing levels of salinization of NaCl, $MgCl_2$ and $CaCl_2$. The salinity was gauged using electrical conductivity (EC). Gypsum was added to one split of these samples before they were treated by the saline solutions. Laboratory reflectance spectra were measured at nadir under a controlled environment using a FieldSpec spectrometer, a 250-W halogen lamp and a Spectralon panel. Variations in spectral reflectance and brightness were evaluated using principal component analysis, as well as the continuum-removed absorption depths of major features at 1450, 1950, 1750 and 2200 nm for both the gypsum-treated (TG) and non-treated (NTG) air-dried soil samples as a function of EC. Pearson's correlation coefficients of reflectance and the band depth with EC were also obtained to establish the relationships with salinity. Results showed that NTG samples presented a decrease in reflectance and brightness with increasing $CaCl_2$ and $MgCl_2$ salinization. The reverse was observed for NaCl. Gypsum increased the spectral reflectance of the soil. The best negative correlations between reflectance and EC were observed in the 1500–2400 nm range for $CaCl_2$ and $MgCl_2$, probably because these wavelengths are most affected by water absorption, as Ca and Mg are much more hygroscopic than Na. These decreased after chemical treatment with gypsum. The most prominent features were observed at 1450,

1950 and 1750 nm in salinized-soil spectra. The 2200-nm clay mineral absorption band depth was inversely correlated with salt concentration. From these features, only the 1750 and 2200 nm ones are within atmospheric absorption windows and can be more easily measured using hyperspectral sensors.

Keywords: soil salinity; remote sensing; spectral reflectance; absorption bands; principal components analysis; electrical conductivity; continuum removal; band depth

1. Introduction

Soil salinization is one of the most relevant and important processes affecting the environmental degradation of land, especially in more arid regions [1]. This is a problem for global agricultural production, because salts slow the growth and development of crops, decreasing productivity. In more severe cases, soil salinization leads to the collapse of agricultural production [2,3]. This is due to the rise in the osmotic potential of the soil solution by the toxic effects of specific ions and by the change in the physical and chemical conditions of the soil [4]. Approximately 30% of irrigated land is moderately or severely affected by salinization [5]. The identification and monitoring of these areas are essential to improving farm management practices [6].

Studies have demonstrated the potential of remote sensing data to detect and map the occurrence and concentration of salts in the soil [1,7,8]. The presence of salts at the terrain surface can be remotely detected directly on bare soils (salt efflorescence and crust) or indirectly through effects on vegetation growth or crop yield [9]. Constraints on the use of remote sensing data for mapping salt affected areas include factors, such as the spectral behavior of salts, the low spectral resolution of some sensor systems, the temporal changes in salinity, the interference of vegetation and the physical and chemical modifications in the soil surface due to salinization [1]. In spite of that, salinity indices have been proposed and tested on images [10,11]. With the improvement in the spectral resolution of image sensors, several studies on reflectance spectroscopy have also been carried out in the laboratory in order to better understand the influence of salts on the spectral response of soils. For example, Howari *et al.* [12] examined the spectral reflectance of soils treated with saline solutions in the laboratory. They observed that the crusts from different salts had diagnostic absorption bands at different wavelengths, whose position did not change with the size of the crystals or the salt concentration. According to them, when gypsum occurred in the treatment solutions of multiple salts, its primary diagnostic features predominated in the spectra of salt crusts. Farifteh *et al.* [13] set up a laboratory experiment involving soils with three textures and six salt minerals to study the relationship between salt concentration in soil and its spectral response. Changes in the shape of absorption bands positioned at wavelengths longer than 1300 nm and in the overall reflectance were observed with increased salt concentration. Furthermore, analysis of continuum-removed spectra indicated a strong negative correlation between soil electrical conductivity (EC) and absorption bands parameters (depth, width and area).

In Brazil, the problems of salinity from irrigation are common in the semi-arid northeast region, but remote sensing studies addressing this topic are rare in the literature. Attempts to use data from the

Moderate Resolution Imaging Spectroradiometer (MODIS/Terra) with coarse spatial resolution (250–500 m spatial resolution for Bands 1–7), which does not allow measurements of narrow absorption bands in saline soil spectra, presented only moderate correlation results between spectral indices and EC [14]. Before using satellite sensors with better spatial and spectral resolutions than MODIS for mapping salinity, laboratory studies are still necessary to analyze the influence of salts on the spectral response of soils from the region.

Studies on the spectral effects of gypsum are also important. Many salinized areas in Brazil are chemically treated with gypsum ($CaSO_4 \cdot 2H_2O$) [15,16], which may affect the spectral response of the other types of salts present on the soil surface [12], but little is known about this. The use of agricultural gypsum as a corrective measure for saline-sodic soils is due to the good solubility of this salt, which reduces aluminum saturation and adds calcium [17]. It is essential in the replacement of sodium, which precipitates as a sulfate and is easily leached with the drainage of water [15].

Figure 1. Location of the study area in northeastern Brazil. Soil samples were collected in the site indicated by the yellow polygon. The color composite (12 September 2013) is from the Operational Land Imager sensor (OLI)/Landsat-8 with Bands 5, 4 and 3 in red, green and blue, respectively.
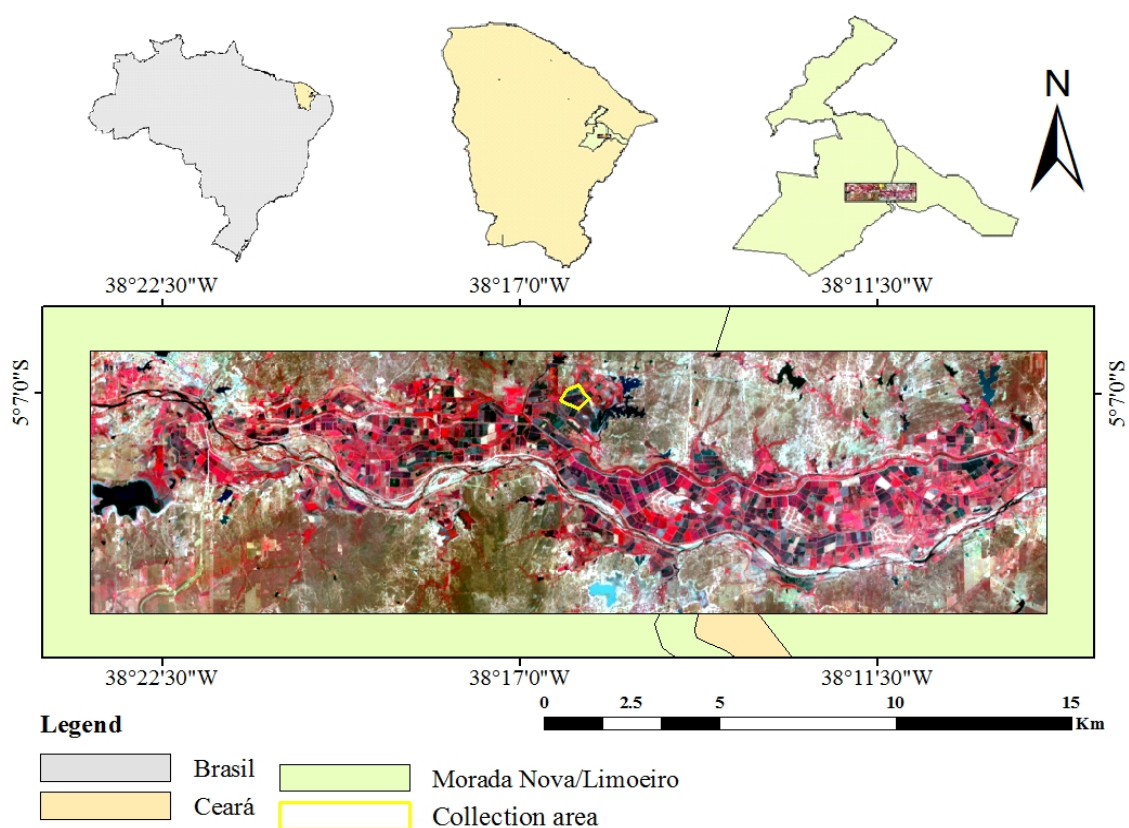
In this study, samples of *Neossolo Flúvico* (fluvent soil in the American soil classification system) with irrigation-induced salinization problems for rice cultivation were collected from salinized areas in the semi-arid region of northeast Brazil (Figure 1). Adopting the general strategy of the experiments by Howari *et al.* [12] and Farifteh *et al.* [18], a laboratory study was carried out to examine variations in spectral reflectance and the depth of the major absorption bands in the salinized-soil spectra. The soils

were treated with different saline solutions of sodium chloride (NaCl), magnesium chloride ($MgCl_2$) and calcium chloride ($CaCl_2$), whose relative concentrations (non-saline to extremely saline) were measured using the EC of the salt solutions. We focused our analysis on the spectral effects of gypsum on local saline soils using principal components analysis and the continuum-removal techniques to observe variations in the spectral reflectance, brightness and depth of the major absorption bands. The implications of the results to mapping and monitoring soil salinization using hyperspectral remote sensing in the region are discussed, in which gypsum may be an indirect indicator of the salinization process, which may affect locally irrigated rice yield.

2. Materials and Methods

2.1. Soil Sample Collection

Soil samples were collected in the less salinized area of the Morada Nova Irrigation district, which is located in the municipalities of Morada Nova and Limoeiro do Norte, in the Brazilian state of Ceará (Figure 1). The natural vegetation of the region is locally known as "Caatinga", which consists primarily of small trees that shed their leaves seasonally. Riparian forest predominates along the main rivers. The relief is relatively flat, with the geology composed mainly of gneisses, migmatites and plutonic rocks of granitic composition. Alluvial soils occur over these rock substrata along the rivers [19]. This area was selected, because it presents many problems of salinization that affect the productivity of irrigated rice [20]. According to the Köppen classification, the climate in the region corresponds to very hot and semi-arid (BSW'h') with average annual rainfall of 600 mm, a mean annual temperature of 27.5 °C and a potential evapotranspiration greater than 2000 mm [21]. The rainy season ranges from January to June, with most of the precipitation concentrated between March and April. Fluvent soils, found in 70% of the irrigated area, were selected for sample collection. These alluvial soils have a texture with typical values of 39% of sand, 33% of silt and 28% of clay [22]. At one specific site of exposed soil (S 5°07'08" and W 38°16'35"; the yellow polygon in Figure 1), 180 samples were collected at a depth of 0 to 15 cm.

2.2. Soil Sample Preparation

An experiment was setup in the laboratory to simulate the accumulation of salts in the soil. Soil samples (180) were crushed and sieved with a 2 mm sieve to reduce the effect of soil particles on the spectra. Soil samples were divided into two sets, each with six replications. One of the six replications was stored for later use/reference, if required.

The first set of samples ("non-treated chemically with gypsum" (NTG)) was placed into polyvinyl chloride (PVC) cylinders, 7.5 cm in diameter by 7.0 cm high, giving a total volume of approximately 309 cm^3 of soil per sample (Figure 2a). This set was treated with salinization by irrigation with distilled water in three saline solutions of NaCl, $MgCl_2$ and $CaCl_2$. Five increasing concentrations of salt or EC levels were used: EC1 (0 dS/m: solution with distilled water only); EC2 (up to 5.48 dS/m); EC3 (5.48 to 9.52 dS/m); EC4 (9.52 to 17.25 dS m); and EC5 (>17.25 dS/m). The EC data (dS/m at 25 °C) were measured with an HI2300 conductivity meter (Hanna Instruments).

The second set of soil samples ("treated chemically with gypsum" (TG)) was treated with 9.4 g/kg of gypsum (50 mesh particle size) and subsequently washed several times with distilled water before being transferred to the containers, following the procedures described by Duarte *et al.* [23]. A simulation of salinization was then carried out using the same procedure described in the previous paragraph.

Thus, each of the two sets involved a total of 75 samples (5 replications × 3 salts × 5 salt concentrations). Once prepared, the soil cylinders were grouped according to their treatment (type of salt and simulated concentration) and placed into plastic trays (Figure 2a,b), where five processes of irrigation by capillarity until saturation were simulated using the saline solutions. A sponge was placed in each tray to ensure the rise of the water table (Figure 2a). All samples were air-dried (natural process of evaporation).

Figure 2. (**a**) The cylinders used in the experimental set-up with a sponge at the bottom; and (**b**) trays with six replications of soil samples per treatment.

(**a**)   (**b**)
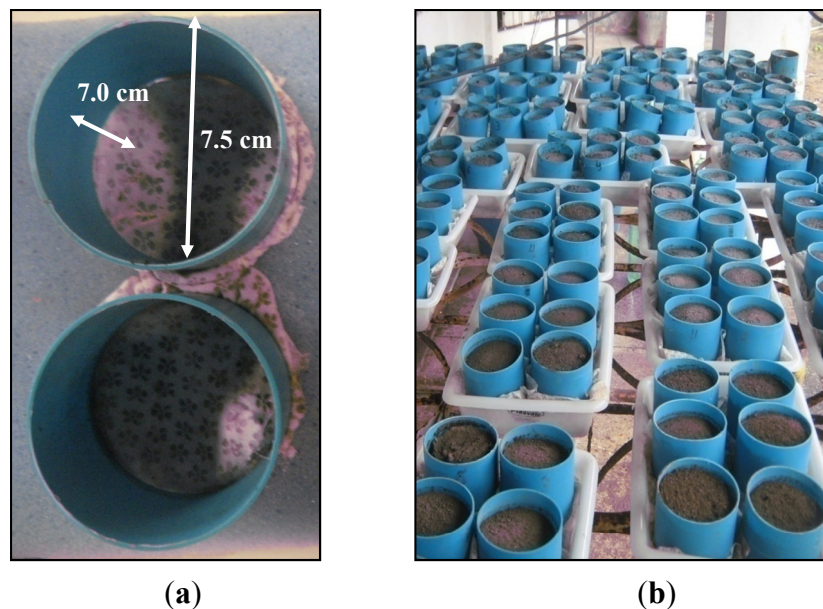
In the soil chemical analyses, the concentration of calcium (Ca^{2+}), magnesium (Mg^{2+}) and sodium (Na^+) in $Mmol/dm^3$ was determined according to the procedures described by Embrapa [24].

2.3. Spectral Data Measurement

To obtain the spectral data in the laboratory, the FieldSpec Pro FR 3 spectrometer was used (Analytical Spectral Devices Inc., Boulder, CO, USA) under a controlled environment (dark room). It has a spectral resolution of 3 nm in the visible and near-infrared region (VNIR = 350–1300 nm), and of 10 nm in the shortwave infrared spectral interval (SWIR = 1300–2500 nm). The sensor was positioned at nadir, 7 cm above the samples. The illumination source was a 250-W halogen lamp with a parabolic reflector, in which the beam was adjusted to a zenith angle of 30°. A calibrated white Spectralon panel was used as a reference. Each reflectance measurement was an average of three readings over the soil.

2.4. Data Analysis

Data analysis included two steps: one to characterize the variations in spectral reflectance and brightness and the other to evaluate the modifications in depth of the major absorption bands with increasing concentration of salts in the soil (or EC) for the NTG and TG samples.

When applied to images, principal components analysis (PCA) is an interesting approach to deal, at the same time, with salt identification and change detection [1]. When applied to laboratory spectra, it also allows a reduction in the data dimensionality and the determination of the factors responsible for the spectral variability in the datasets [25]. The eigenvalues indicate the number of PCs responsible for most of the data variance, whereas the eigenvectors indicate the most important input variables to explain each component. As part of the first step in data analysis, PCA was applied separately for each salt to both datasets (NTG and TG). Reflectance values of the whole spectrum were used as input variables. Components with eigenvalues greater than one were retained and their eigenvectors analyzed in order to verify the contribution of each wavelength reflectance to explain each component. Principal components scores were plotted as a function of EC for the NTG and TG samples. Based on these scores and on the significance of the PCs, spectra were selected and compared to each other to show variations in reflectance with the increase in salt concentration. Pearson's correlation coefficients between reflectance and EC were also obtained to establish the relationships with salinity.

In the second step, in order to filter out the absorption bands from spectra and to quantify the changes in depth of the major absorption bands, the continuum removal technique was used [26]. This technique consists in the division of the original reflectance values ($\rho\lambda$original) on each wavelength (λ) by the corresponding values projected on the straight line ($\rho\lambda$continuum) connecting the ends of a given absorption band. The depth of an absorption band (D) centered at a given wavelength, λ_c, is calculated by Equation (1) [26]:

$$D = 1 - \frac{\rho_{\lambda c \, original}}{\rho_{\lambda c \, continuum}} \tag{1}$$

In principle, the larger D becomes for a given λ, the greater the amount of the absorber. The values of D for the major absorption bands were then plotted as a function of EC for the NTG and TG samples, and the correlations were analyzed.

3. Results and Discussion

3.1. Soil Chemical Properties

The average values of Ca^{2+}, Mg^{2+} and Na^+, measured from the 150 samples of the different salt concentrations (EC classes), are shown in Table 1. These analyses were made after the spectral measurements taken in the laboratory to take into account possible physico-chemical modifications in the soil surface with salinity. The results for EC1 in the NTG set of samples showed that the original soil, irrigated with distilled water, was already slightly to moderately saline, with EC values varying from 4.6 ($CaCl_2$) to 6.2 (NaCl) dS/m. As expected, the application of gypsum caused significant increases of calcium in the samples. For example, in the case of $CaCl_2$ and EC5, the values ranged

from 628.7 to 1613.9 Mmol/dm^3 (Table 1). However, because of handling-difficulties in the laboratory (limited drainage), the application of gypsum did not significantly reduce the EC.

Table 1. Average values of the chemical attributes for non-treated (NTG) and treated (TG) soil samples with gypsum, as a function of salt concentration, expressed by electrical conductivity (EC).

	Attribute	Electrical Conductivity (EC)									
		EC1		EC2		EC3		EC4		EC5	
		NTG	TG	NTG	TG	NTG	TG	NTG	TG	NTG	TG
NaCl	EC (dS/m)	6.2	6.9	18.6	34.5	35.7	40.7	49.6	64.9	112.8	138.9
	Na$^+$ (Mmol/dm^3)	60.7	20.7	132.7	76.8	269.5	141.3	322.4	245.4	1101.3	486.5
MgCl$_2$	EC (dS/m)	5.6	4.8	19.3	16.9	38.3	24.6	76.3	49.3	98.8	97.8
	Mg^{2+} (Mmol/dm^3)	109.8	89.2	154.5	163	189.7	209.3	208.5	234.3	235.7	239.5
CaCl$_2$	EC (dS/m)	4.6	5.2	15	15.5	32	29.6	76.3	51.2	101.9	103.8
	Ca^{2+} (Mmol/dm^3)	142.8	791.4	211.1	819.4	251.9	920.7	444.1	1015	628.7	1,613.9

3.2. Spectral Data Analysis

The reflectance spectra of the pure salts used in the laboratory experiment are shown in Figure 3. The salts were previously dried in an oven at 105 °C for two hours. In the reflectance curve of gypsum, absorption bands around 1450 nm, 1750 nm, 1950 nm and 2200 nm can be observed. Bands located near 1450 nm and 1950 nm are produced by water molecules [12,18]. The 2200 nm absorption is caused by combination tones (stretch and bend vibrations) of octahedral coordinated hydroxyl groups in dioctahedral silicates [12,27,28]. The NaCl showed a higher reflectance in the VNIR and shortwave infrared (SWIR) compared to the other salts, and only two well-defined absorption bands at 1450 nm and 1950 nm, which are related to fluid inclusions and/or absorbed water [6,12]. In the MgCl$_2$ spectrum, there were strong features close to 975 nm and 1200 nm, followed by a strong reflectance decrease from 1400 to 2500 nm. The wavelength position of these features is related to the bonding effects of the water molecules [27]. When compared to the other salts, the reflectance of the MgCl$_2$ decreased strongly from 1900 nm, which was also observed by Farifteh *et al.* [18]. The CaCl$_2$ spectrum showed strong absorption bands around 950 nm, 1200 nm, 1450 nm, 1750 nm and 1950 nm, with a weaker band around 2200 nm. MgCl$_2$ and CaCl$_2$ are much more hygroscopic than NaCl. During the salinization experiment, they may absorb moisture from the air, which may affect the SWIR reflectance and the appearance of some water absorption bands when compared to NaCl.

3.3. Effects of EC on the Spectra for NTG and TG Soils

Principal components analysis of the spectral data showed that the first component accounts for 61.01%, 81.37% and 73.11% of the total variance for the NaCl, MgCl$_2$ and CaCl$_2$ samples, while the second component accounts for 33.16%, 13.71% and 20.69% of the variance of the same sample suites. The corresponding weightings for the first principal component (Figure 4a) show similar behavior for all salt treatments, with large weightings for all wavelengths, except for within narrow bands, especially at 1950 nm and 2500 nm (the edge of fundamental stretch vibration of water

centered at 2700 nm), both related to water content, and to a lesser degree at 2200, 1700, 1650, 1550 and 1450 nm, presumably reflecting variations in gypsum content. As illustrated in Figure 5, PC1 expressed variations in brightness (overall reflectance) of the samples or in average reflectance ($\rho b1 + \rho b2 + ... + \rho bn/n$ bands) for the spectral range studied, because it presents large loading values for most of the wavelengths. On the other hand, PC2 displayed negative weighting factors in the VNIR and positive ones in the SWIR, expressing variations in the shape of the spectra and in the absorption bands of the salts (Figure 4b).

Figure 3. Reflectance spectra of the salts and gypsum used in the experiment. The positions of major absorption features are indicated by arrows.
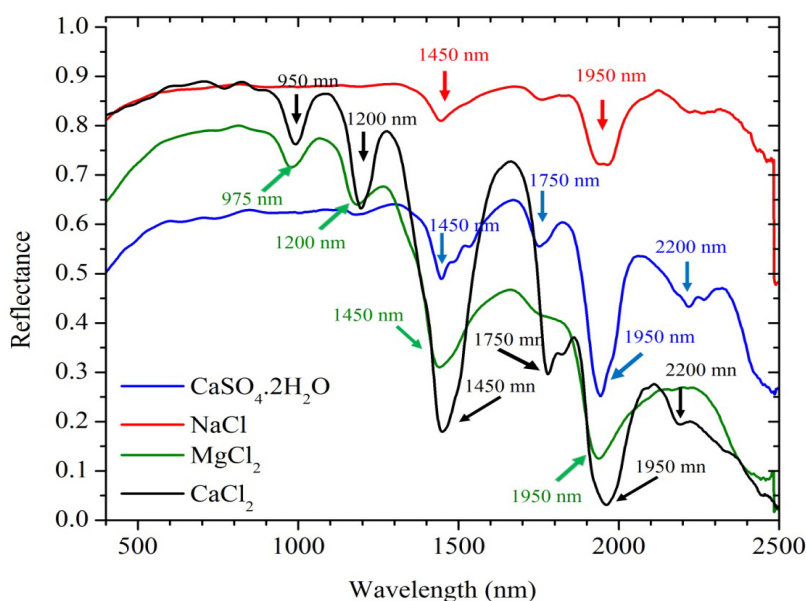
Figure 4. Weighting factors of the first (**a**) and second (**b**) principal components (PC1 and PC2).

(**a**)   (**b**)
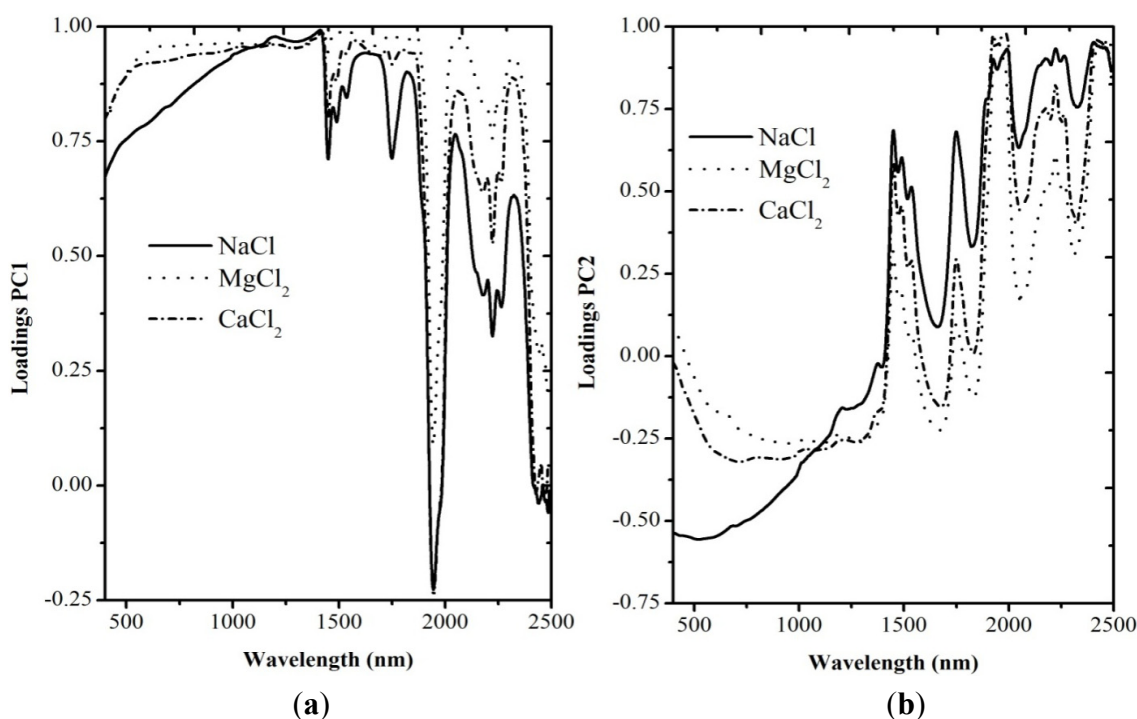
Figure 5. The relationship between the average soil reflectance in the 400–2400 nm range and the first principal components scores (PC1) for NaCl samples chemically treated with gypsum (TG).
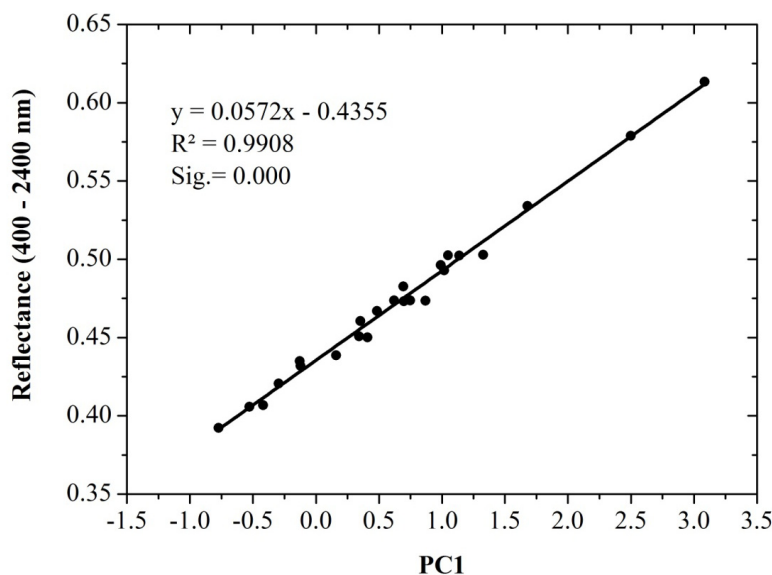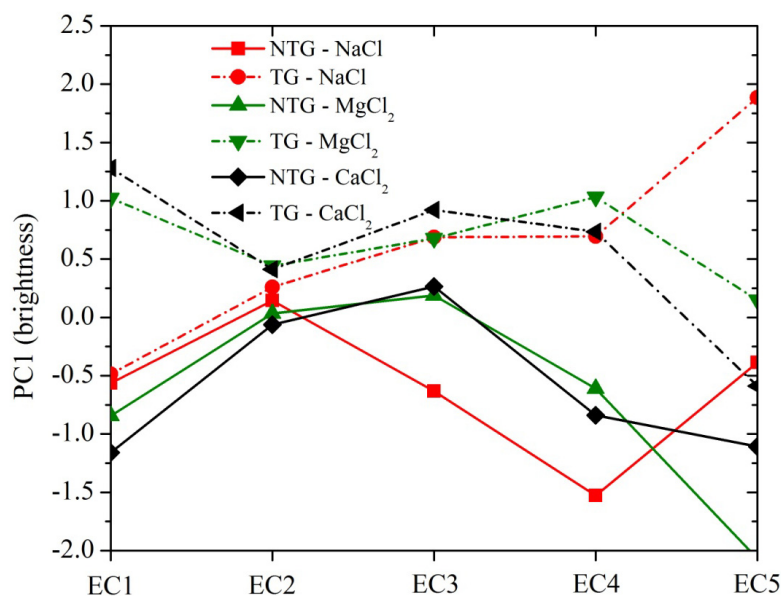

Figure 6. Projection of average PC1 scores for untreated (NTG) and treated (TG) soil samples with gypsum, as a function of the five classes of electrical conductivity (EC) of the saline solutions used to irrigate the soil.


The projection of average PC1 scores for the NTG and TG samples of the three salts showed that the samples treated chemically with gypsum (dashed lines in Figure 6) had higher PC1 scores than those of the untreated samples (solid lines). The magnitude of the spectral influence of gypsum depends on the type and concentration of salts in the mixture [12]. The brightness of the NaCl samples (TG) increased from EC1 to EC5, as expressed by the gradual increase in the PC1 scores (Figure 6). The reverse was verified for $CaCl_2$ and $MgCl_2$, whose spectral reflectance decreased strongly from the VNIR to SWIR, also due to the highly hydroscopic nature of these salts (Figure 3). Inspection of the

reflectance spectra of soil samples salinized with NaCl (Figure 7a) and MgCl$_2$ (Figure 7b) indicated that the patterns of increasing and decreasing brightness in the PC space of Figure 6, under chemical treatment with gypsum, were consistent with the SWIR reflectance increase for NaCl and with the VNIR reflectance decrease for MgCl$_2$ from EC1 to EC5, respectively. Furthermore, the spectral features of gypsum prevailed over those of NaCl and MgCl$_2$.

For the NTG samples, except for NaCl, the brightness of the other two salts first increased from EC1 to EC3 (higher PC1 scores) and then decreased towards EC5 (Figure 6). The decrease in brightness with salt concentration for MgCl$_2$ (NTG) in Figure 6 was consistent with results obtained by Farifteh *et al.* [18] when calculating the normalized albedo (1000–2400 nm) of three types of soils irrigated with saline solutions compared to the same soils irrigated only with distilled water. For NaCl (NTG), the results of Farifteh *et al.* [18] varied with the soil type or texture.

Figure 7. Spectral variation with electrical conductivity (EC) showing higher and lower reflectance values from EC1 to EC5 for (**a**) NaCl and (**b**) MgCl$_2$, respectively.

(**a**)   (**b**)
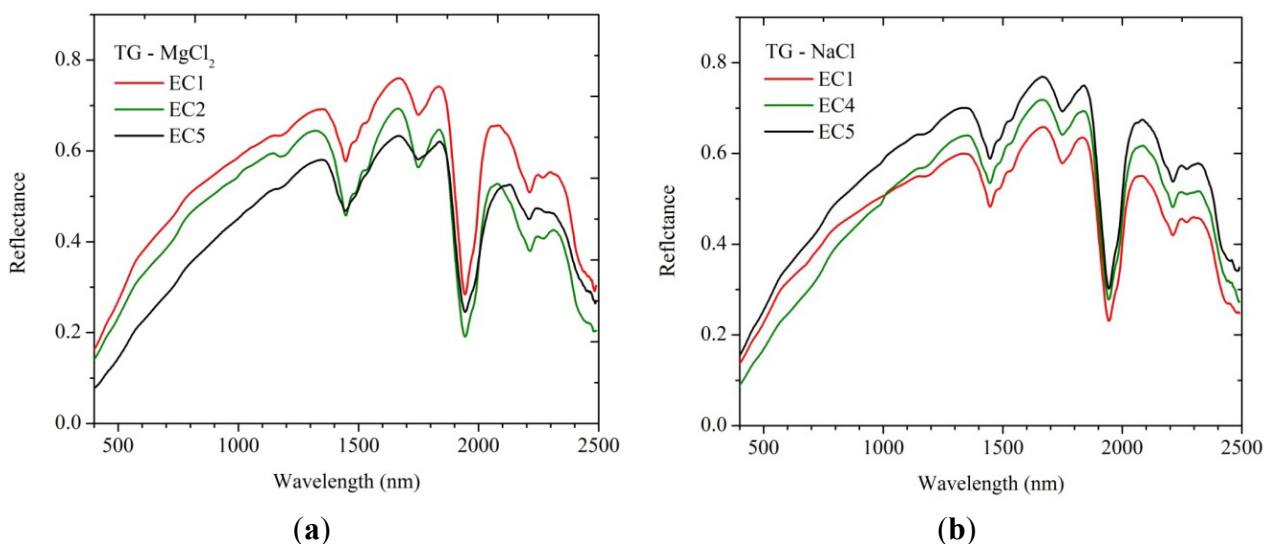
3.4. Relationship of EC with Spectral Reflectance for NTG and TG Soils

NaCl presented positive correlation results with EC in the SWIR. Strong negative correlations were observed in the spectra of the fluvent soils salinized with MgCl$_2$ and CaCl$_2$ under NTG between 1400 and 2400 nm (Figure 8). In the work by Farifteh *et al.* [18], MgCl$_2$ was also the salt that showed the best negative correlations with reflectance in the SWIR. Results shown in Figure 8 were also consistent with the spectral response of these two salts, which showed a significant reduction in reflectance from the VNIR to SWIR (Figure 3). The correlation coefficients (*r*) decreased significantly in the SWIR for the TG set of samples, with the gypsum producing a reduction in the *r* values of −0.91 to +0.42 for MgCl$_2$ and of −0.93 to +0.11 for CaCl$_2$ at 1950 nm.

Inspection of the scatterplots between reflectance at 1950 nm and EC (soil salinity) showed linear relationships for the three salts (Figure 9). However, detailed inspection of Figure 9a for NaCl showed inverse and poor correlations between the reflectance at 1950 nm and EC, because this wavelength comprises a well-defined absorption band observed in the NaCl spectrum (Figure 3).

Figure 8. Pearson's correlation coefficients for the relationship between spectral reflectance and electrical conductivity (soil salinity) for NTG soil samples (*n* = 25 per salt).
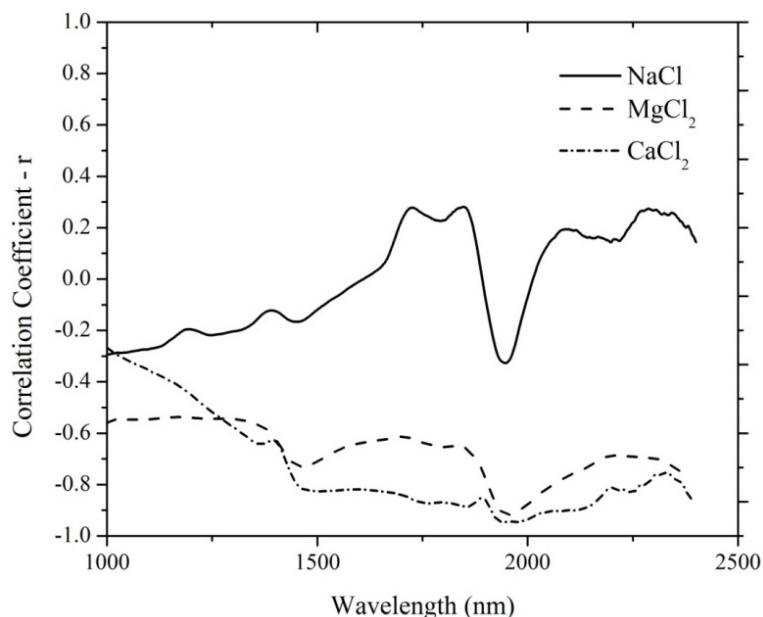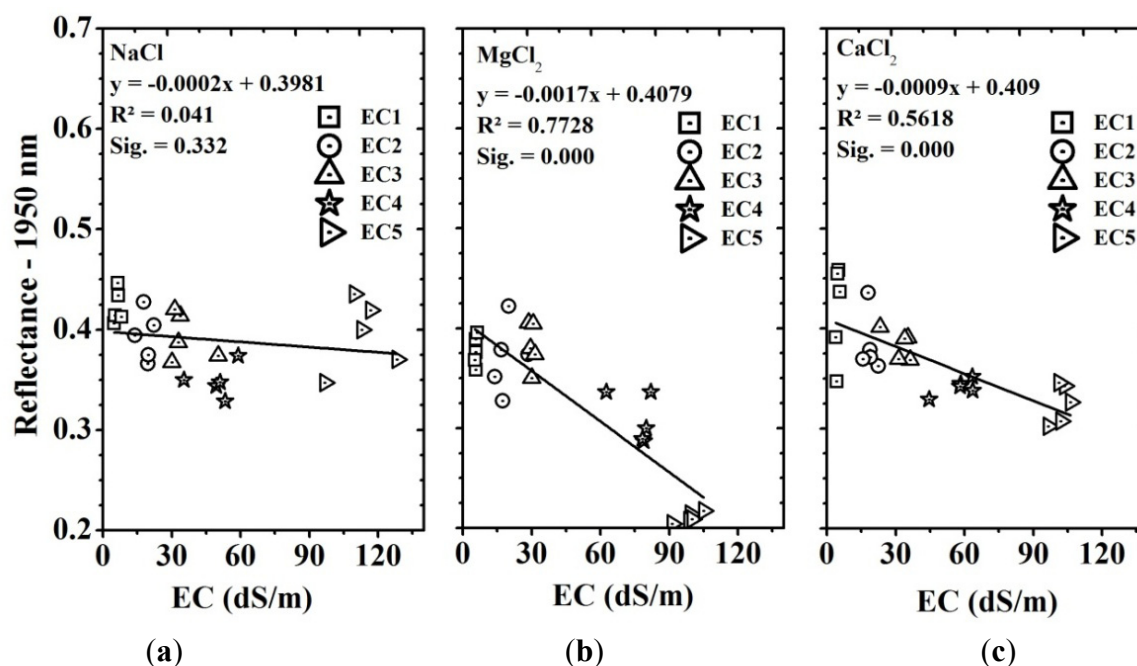

Figure 9. Relationship between the reflectance at 1950 nm and the electrical conductivity (EC) of the soil samples salinized with (**a**) NaCl; (**b**) MgCl$_2$ and (**c**) CaCl$_2$.

3.5. Relationship of Band Depth with EC for NTG and TG Soils

When compared with the pure salt spectra (Figure 3), the NTG and TG spectra of the fluvent soils salinized in the laboratory showed less intense well-defined spectral features. The deepest absorption bands, calculated using the continuum removal method, were observed at 1450 nm, 1950 nm and 1750 nm. The features at 2200 nm for NTG samples are due to the presence of clay minerals in the soils [7]. They are approximately coincident with the gypsum feature (Figure 10).

Figure 10. Alluvial soil spectra of EC1 samples treated (TG) and non-treated (NTG) with gypsum.
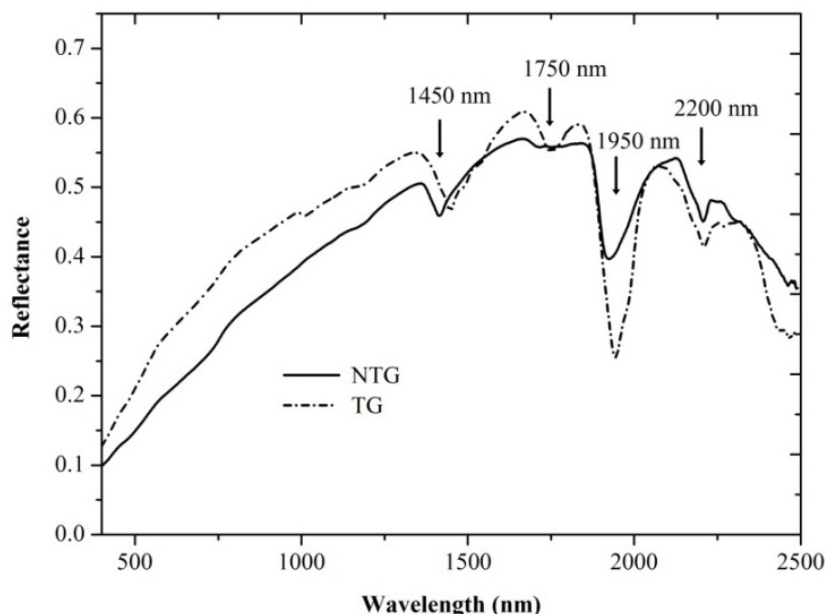
In arid and semi-arid regions, NaCl is present in greater quantities compared to the other studied salts, mostly occurring in the form of crystals or efflorescence resulting from the evaporation of salinized water [18]. For the NTG samples (Figure 11a,c,e), $MgCl_2$ presented better-defined absorption bands at 1450 nm and especially at 1950 nm when compared with NaCl and $CaCl_2$. The depth values of these bands were positively and highly correlated with the concentration of this salt, expressed by the increasing values of EC (Figure 12). This same trend was observed by Weng *et al.* [29], who found a relationship between the concentration of this salt and the depth of this absorption band. The correlation results for NaCl and $CaCl_2$ were lower than those for $MgCl_2$, probably because this salt is much more hygroscopic than the others.

In general, the TG Samples (Figure 11b,d,f) presented deeper absorption bands than those observed for the NTG samples (left side of Figure 11), due to the spectral influence of the gypsum. The presence of an additional feature, centered at 1750 nm and seen in the gypsum spectrum in Figure 3, confirms the spectral effects of the gypsum used in the chemical treatment of the samples for the correction of salinization.

Under both soil conditions (NTG and TG), the 2200 nm clay mineral absorption bands in soil spectra were less evident and less deep when the samples became more saline (Figure 11). Inverse correlations between the depth of the 2200 nm absorption band and the EC values were observed for both TG and NTG (Figure 13). According to Dehaan and Taylor [7], the reduction in depth of this band may occur as a result of the loss of crystallization of the clayey minerals, due to the salinization process. Obviously, gypsum has a feature in an approximately spectral position, which affects the appearance of the clay mineral absorption.

Figure 11. Changes in average depth and standard deviation of the major absorption bands present in the reflectance spectra of the NTG (**left**) and TG (**right**) samples of fluvent soil for different salts (NaCl, MgCl$_2$ and CaCl$_2$) and electrical conductivity (EC) levels.
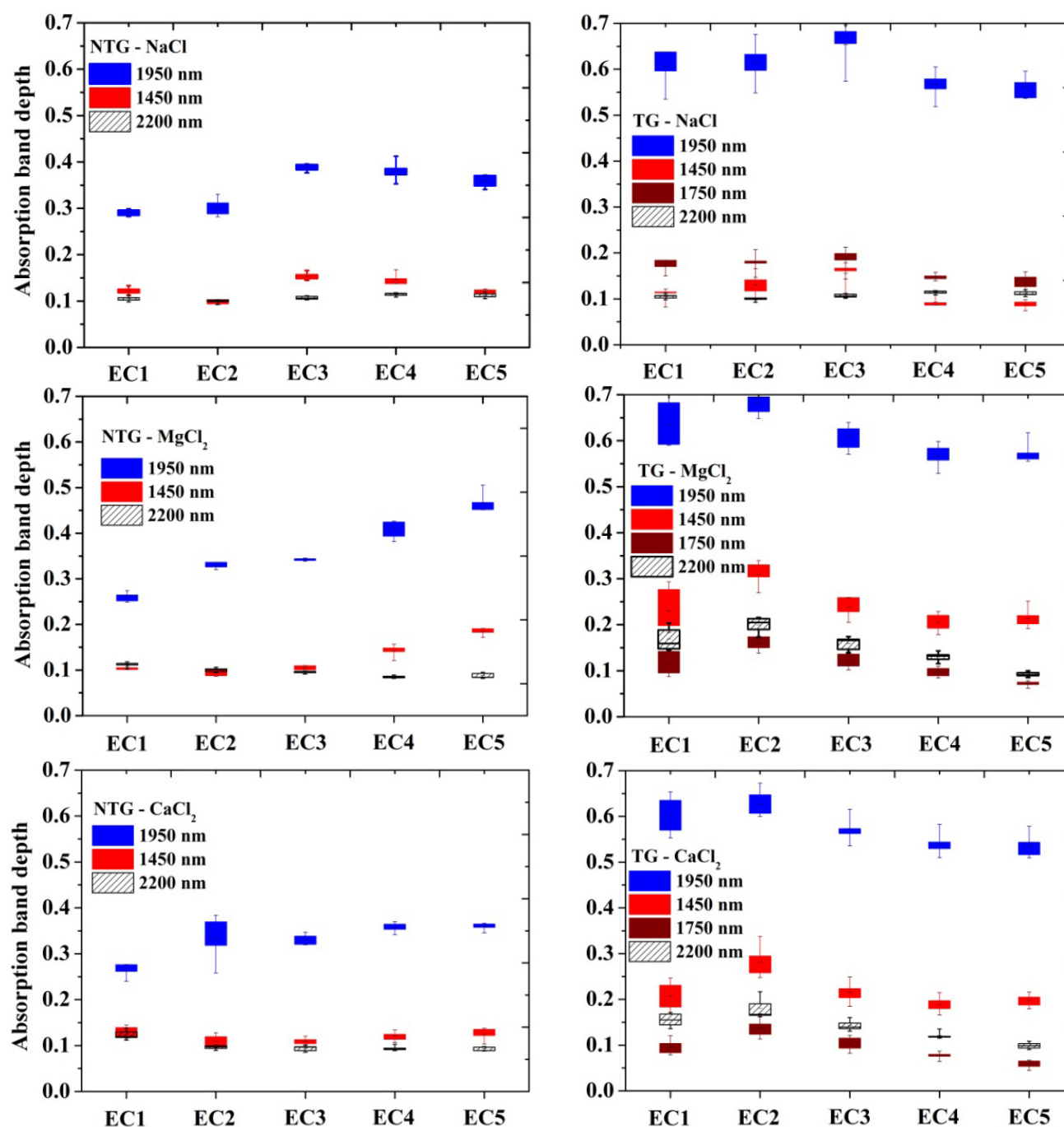
Figure 12. The relationship between the depths of the absorption bands centered at 1450 nm and 1950 nm and the values of electrical conductivity (EC) for MgCl$_2$ salinization. Results refer to samples non-treated chemically with gypsum (NTG).
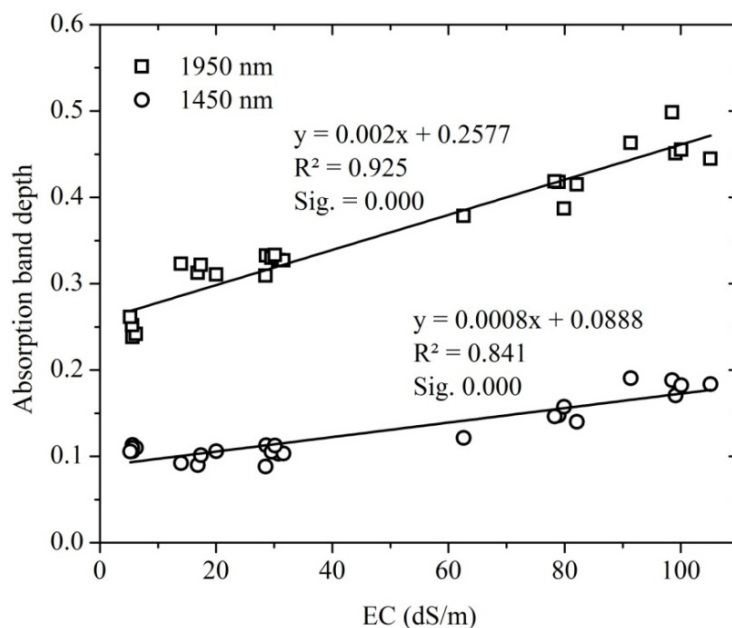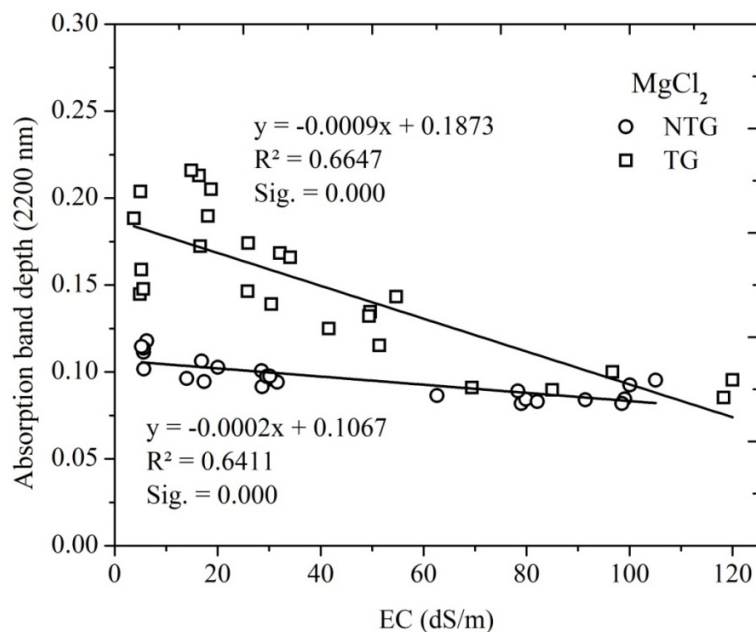

Figure 13. Relationship between the depth of the 2200 nm clay mineral absorption band and electrical conductivity (EC) for MgCl$_2$ salinization for NTG and TG samples.

4. Conclusions

Brazilian alluvial soil samples were treated in the laboratory with increasing salinization levels of NaCl, MgCl$_2$ and CaCl$_2$, and the spectral effects of gypsum, a corrective for saline soils, were studied. Results showed that the spectral reflectance and brightness of the NTG samples of fluvent soil decreased from EC1 (non-saline solution with distilled water) to EC5 (extremely saline solution) for

$CaCl_2$ and $MgCl_2$. The opposite was observed for NaCl. Under chemical treatment with gypsum, the brightness of the TG samples increased for all salts compared to the NTG samples.

In the set of NTG samples, the best correlations between reflectance and soil salinity, expressed as EC values, were obtained for $CaCl_2$ and $MgCl_2$ in the 1500–2400 nm spectral interval. Chemical treatments with gypsum affected these relationships, reducing the SWIR correlation results.

For the absorption bands of the pure-salt spectra, the best-defined features seen in the spectra of the salinized fluvent soils were those at 1450 nm and 1950 nm. After treatment with gypsum, additional absorption features centered at 1750 nm for this constituent were also observed. Strong positive correlations between the depths of the absorption bands positioned at 1450 nm and 1950 nm and the EC values were only seen for the $MgCl_2$, probably because this salt is much more hygroscopic than the others. The depth of the 2200 nm clay mineral absorption band present in soil spectra, which was approximately coincident with the gypsum feature, was inversely correlated with the EC values.

The results of this laboratory experiment have implications on salinization investigations in the study area with future hyperspectral sensors, such as the EnMAP (Environmental Mapping and Analysis Program) or HyspIRI (Hyperspectral Infrared Imager), with spatial resolutions of 30 m and 60 m, respectively, and more than 200 bands. The absorption bands at 1450 nm and 1950 nm coincide with spectral intervals of strong absorption by atmospheric water vapor, but the feature at 1750 nm can be detected in the pixel spectra of exposed salinized soils. This feature occurs in the spectra of gypsum, a corrective for saline soils that can be used indirectly to map salinization. Detection of modifications in the depth of the 2200 nm clay mineral absorption band due to salinization or the use of gypsum depends strongly on the instrumental signal-to-noise ratio (SNR) in the SWIR. Because gypsum and the other studied salts are much stronger absorbers in the SWIR due to their different hygroscopic nature, the use of VNIR/SWIR indices can be also helpful for mapping salinity.

Author Contributions

Luis Clenio J. Moreira and Adunias dos Santos Teixeira designed and performed the experiments. All the authors contributed equally in the data analysis and in the manuscript preparation.

Conflicts of Interest

The authors declare no conflict of interest in conducting this study.

References

1. Metternicht, G.I.; Zinck, J.A. Remote sensing of soil salinity: Potentials and constraints. *Remote Sens. Environ.* **2003**, *85*, 1–20.
2. Lal, R. Soils and food sufficiency. A review. *Agron. Sustain. Dev.* **2009**, *29*, 113–133.
3. D'Odorico, P.; Bhattachan, A.; Davis, K.F.; Ravi, S.; Runyan, C.W. Global desertification: Drivers and feedbacks. *Adv. Water Resour.* **2013**, *51*, 326–344.
4. Santana, M.J.; Carvalho, J.A.; Silva, E.L.; Miguel, D.S. Efeito da irrigação com água salina em um solo cultivado com feijoeiro (*Phaseolus vulgaris L.*). *Ciência Agrotecnológica* **2003**, *27*, 443–450.
5. Food and Agriculture Organization (FAO). *Crops and Drops: Making the Best Use of Water for Agriculture*; FAO: Rome, Italy, 2002; p. 28
6. Wang, Q.; Pingheng, L.; Chen, X. Modeling salinity effects on soil reflectance under various moisture conditions and its inverse application: A laboratory experiment. *Geoderma* **2012**, *170*, 103–111.
7. Dehaan, R.; Taylor, G.R. Image-derived spectral endmembers as indicators of salinization. *Int. J. Remote Sens.* **2003**, *24*, 775–794.
8. Yao, Y.; Ding, J.L.; Kelimul, A.; Zhang, F.; Lei, L. Research on remote sensing monitoring of soil salinization based on measured hyperspectral and EM38 data. *Spectrosc. Spectr. Anal.* **2013**, *33*, 1917–1921.
9. Mougenot, B.; Epema, G.F.; Pouget. M. Remote sensing of salt affected soils. *Remote Sens. Rev.* **1993**, *7*, 241–259.
10. Weng, Y.L.; Gong, P.; Zhu, Z.L. A spectral index for estimating soil salinity in the Yellow River Delta Region of China using EO-1 Hyperion data. *Pedosphere* **2010**, *20*, 378–388.
11. Wang, F.; Chen, X.; Luo, G.; Ding, J.; Chen, X. Detecting soil salinity with arid fraction integrated index and salinity index in feature space using Landsat TM imagery. *J. Arid Land* **2013**, *05*, 340–353.
12. Howari, F.M.; Goodell, P.C.; Miyamoto, S. Spectral properties of salt crusts formed on saline soils. *J. Environ. Qual.* **2002**, *31*, 1453–1461.
13. Farifteh, J.; Farshad, A.; George, R.J. Assessing salt-affected soils using remote sensing, solute modelling, and geophysics. *Geoderma* **2006**, *130*, 191–206.
14. Bouaziz, M.; Matschullat, J.; Gloaguen, R. Improved remote sensing detection of soil salinity from a semi-arid climate in Northeast Brazil. *Comptes Rend. Geosci.* **2011**, *343*, 795–803.
15. Melo, R.M.; Barros, M.F.C.; dos Santos, P.M.; Rolim, M.M. Correção de solos salino-sódicos pela aplicação de gesso mineral. *Revista Brasileira de Engenharia Agrícola e Ambiental.* **2008**, *12*, 376–380.
16. Lacerda, C.F.; Souza, G.G.; Silva, F.L.B.; Guimarães, F.V.A.; Silva, G.L.; Cavalcante, L.F. Soil salinization and maize and cowpea yield in the crop rotation system using saline waters. *Eng. Agrícola.* **2011**, *31*, 663–675.
17. Caires, E.F.; Fonseca, A.F.; Mendes, J.; Chueiri, W.A.; Madruga, E.F. Produção de milho, trigo e soja em função das alterações das características químicas do solo pela aplicação de calcário e gesso na superfície, em sistema de plantio direto. *R. Bras. Ci. Solo* **1999**, *23*, 315–327.

18. Farifteh, J.; van der Meer, F.; van der Meijde, M.; Atzberger, C. Spectral characteristics of salt-affected soils: A laboratory experiment. *Geoderma*. **2008**, *145*, 196–206.

19. Souza, M.J.N. Geomorfologia. In *Instituto de Planejamento do Estado do Ceará—IPLANCE*. Atlas do Ceará: Fortaleza, Brazil, 1997; pp. 18–19.

20. Fraga, T.I.; Carmona, F.C.; Anghinoni, I.; Genro Junior, S.A.; Marcolin, E. Flooded rice yield as affected by levels of water salinity in different stages of its cycle. *R. Bras. Ci. Solo*. **2010**, *34*, 175–182.

21. Barbosa, F.C.; Teixeira, A.S., dos; Gondim, R.S. Espacialização da evapotranspiração de referência e precipitação efetiva para estimativa das necessidades de irrigação na região do Baixo Jaguaribe—CE. *Revista Ciência Agronômica*. **2005**, *36*, 24–33.

22. Cunha, C.S.M. *Relação entre Solos Afetados por sais e Concentração de Metais Pesados em Quatro Perímetros Irrigados no Ceará. Master Dissertation*; Universidade Federal do Ceará (UFC): Fortaleza, Brazil, 2013.

23. Duarte, S.N.; Dias, N.S.; Teles Filho, J.F. Recuperação de um solo salinizado devido ao excesso de fertilizantes em ambiente protegido. *Irriga* **2007**, *12*, 422–428.

24. Embrapa—Empresa Brasileira de Pesquisa Agropecuária. *Centro Nacional de Pesquisa dos Solos*. Manual de Métodos de Análise de solo: Rio de Janeiro, Brazil, 1997; p. 212.

25. Moreira, R.C.; Galvão, L.S. Variation in spectral shape of urban materials. *Remote Sens. Lett.* **2010**, *1*, 149–158.

26. Clark, R.N.; Roush, T.L. Reflectance spectroscopy: Quantitative analysis techniques for remote sensing applications. *J. Geophys. Res*. **1984**, *89*, 6329–6340.

27. Hunt, G.R.; Salisbury, J.W.; Lenhoff, C.J. Visible and near-infrared spectra of minerals and rocks. II. Carbonates. *Mod. Geol.* **1971**, *2*, 23–30.

28. Pastor, I.M.; Pedreño, J.N.; Koch, M.; Gómez, I. Applying imaging spectroscopy techniques to map saline soils with ASTER images. *Geoderma* **2010**, *158*, 55–65.

29. Weng, Y.; Gong, P.; Zhu, Z. Reflectance spectroscopy for the assessment of soil salt content in soils of the Yellow River Delta of China. *Int. J. Remote Sens*. **2008**, *29*, 5511–5531.